Journal of Geosciences and Geomatics, 2019, Vol. 7, No. 4, 157-171
Available online at http://pubs.sciepub.com/jgg/7/4/1
Published by Science and Education Publishing
DOI:10.12691/jgg-7-4-1

Petrophysical Evaluation and Reservoir Geometry Deduction of Idje Field, Offshore Niger Delta Nigeria

Ukuedojor Kingsley Oghenemeruo, Maju-Oyovwikowhe Gladys Efetobore*

Department of Geology, Faculty of Physical Sciences, University of Benin, P.M.B. 1154 Benin City, Edo State, Nigeria
*Corresponding author: efetobore.maju@uniben.edu

Received May 11, 2019; Revised June 26, 2019; Accepted July 04, 2019

Abstract The reservoir properties of the D-3 sandstone in Idje field of the Niger Delta region had been established. Petrophysical evaluation had been carried out as well as deducing the reservoir geometry. Idje field is an 8.4 km^2 area between latitudes 4^{o}31'49"N and 4^o 33'23" N and longitudes 4^{o}34'43"E and 4^{o}36'17"E offshore Niger Delta in water depth of approximately 1000m on the continental slope. Well logs suites from ten wells comprising gamma ray, resistivity, neutron and density were obtained and analyzed. Petrophysical parameters were derived from which deductions and interpretations were made based on findings. Three sets of correlations were made on the E-W, NE-SW and NW-SE trends to ascertain the geometry of the reservoir. From the result, it was observed that the reservoir was a sedimentary dome possibly resulting from an underlying shale diapir. The log motif range from cylindrical shape with sharp base and top in the western portion to serrated shape in the eastern portion indicating a gradual transition from a slope channel fill (probably submarine canyon) in the proximal west to a distal deep marine slope towards the East. The Vshale range of 0.02 to 0.14 was shown to be for very clean sandstone in the west to slightly shaly sandstone in the east. The reservoir was shown to have a very good porosity and excellent permeability with average porosity value of 0.25 and an average permeability value of 3393.69m. Average hydrocarbon saturation of 48% was observed. Irreducible water saturation was 8% and the average water saturation across the hydrocarbon penetrated wells was 52%. Based on the aforementioned, water would be produced in the field alongside hydrocarbon and therefore possible measures for separation must be employed.

Keywords: *petrophysical evaluation, reservoir geometry, reservoir properties, Idje field, Niger Delta*

Cite This Article: Ukuedojor Kingsley Oghenemeruo, and Maju-Oyovwikowhe Gladys Efetobore, "Petrophysical Evaluation and Reservoir Geometry Deduction of Idje Field, Offshore Niger Delta Nigeria." *Journal of Geosciences and Geomatics*, vol. 7, no. 4 (2019): 157-171. doi: 10.12691/jgg-7-4-1.

1. Introduction

Proper understanding of the underlying geology helps to accurately predict the hydrocarbon potentials and reserves estimation of a petroleum field. Information gathered from cores, seismic, well logs and Biostratigraphic data help to resolve this underlying geology and thus aid in characterizing the hydrocarbon reservoir. Reservoir characterization therefore is the quantification, integration, reduction and analysis of geological, petrophysical, seismic and engineering data. Reservoirs in the Niger Delta exhibit a wide range of complexities in their sedimentological and petrophysical characteristics due to differences in hydrodynamic conditions prevalent in their depositional settings. Petrophysics therefore plays a fundamental role in the description, characterization and evaluation of reservoirs. It is always essential to integrate petrophysical data with geological and engineering data to accurately predict reservoir quality. Reserve estimation therefore is based on the field wide distribution of these reservoir properties. Due to the intense petroleum exploration and exploitation activities in the Niger Delta region during the last two decades, a vast amount of data have been accumulated from which it had been possible to establish the historical reconstruction and evolution of the Niger Delta basin [1,2].

Ten wells were drilled in the Idje field to produce the D-3 reservoir; Idje 2, 3 and 10 penetrated the gas and oil zones; Idje 1 penetrated only the oil zone. Idje 4 and 6 penetrated the fringe of the reservoir while Idje 5, 7, 8 and 9 are dry wells which penetrated only the water zone. Well logs were obtained and correlated across the D-3 reservoir. Also, the petrophysical characteristic of the D3 reservoir was determined. Increased confidence in the reservoir characterization and architecture is provided by the integration of the large number of well data. The objective of this study is to provide a better understanding of the distribution pattern of the reservoir properties across the field. This study covers the evaluation of petrophysical properties from well logs. Reservoir geometry and architecture was interpreted from structural correlation covered by this study. It also attempts an interpretation of environment of deposition using the gamma ray log motifs. It tends to characterize the D-3 reservoir across the entire field with respect to the reservoir properties. Finally, a computation of the field reserve was done. Ultimately, this study will help to perform an accurate reservoir evaluation.

1.1. Location and Geology of the Study Area

Idje is a fictitious field name given to an 8.4 km^2 area between latitudes 4°31'49"N and 4° 33'23" N and longitudes 4°34'43"E and 4°36'17"E offshore Niger Delta in water depth of approximately 1000m on the continental slope and it lies at approximately 170km southwest of Warri as seen in Figure 1 and Figure 2 respectively.

Figure 1. Map extract from Microsoft Encarta, 2007 showing study location

Figure 2. Map extract from Google Earth showing project location on continental slope

1.2. The Niger Delta Regional Setting

The Niger Delta covers a 70,000 square kilometer area within the Gulf of Guinea, West Africa. Although the modern Niger Delta formed in the Early Tertiary, sediments began to accumulate in this region during the Mesozoic rifting associated with the separation of the Africa and South American continents [3,4,5]. Synrift marine clastics and carbonates accumulated during a series of transgressive and regressive phases between the Cretaceous to Early Tertiary; the oldest dated sediments are Albian age [5]. These synrift phases ended with basin inversion in the Late Cretaceous (Santonian). Proto-Niger Delta regression continued as continental margin subsidence resumed at the end of the Cretaceous (Maastrichtian). Niger Delta progradation into the Gulf of Guinea accelerated from the Miocene onward in response to evolving drainages of the River Niger, River Benue and Cross River and continued continental margin subsidence. Tertiary Niger Delta deposits are characterized by a series of Depobelts that strike northwest- southeast, sub-parallel to the present day shoreline. Depobelts become successively younger basinwards, ranging in age from Eocene in the north to Pliocene offshore of the present shoreline. Depobelts, tens of kilometres wide, are bounded by a growth fault to the north and a counter regional fault seaward. Each sub-basin contains a distinct shallowing upward depositional cycle with its own tripartite assemblage of marine, paralic, and continental deposits. Depobelts define a series of punctuations in the progradation of this deltaic system. As deltaic sediment loads increase, underlying delta front and prodelta marine shale begin to move upward and basinwards. Mobilization of basal shale caused structural collapse along normal faults, and created accommodation for additional deltaic sediment accumulation. As shale withdrawal nears completion, subsidence slows dramatically, leaving little room for further sedimentation. As declining accommodation forces a basinwards progradation of sediment, a new depocenter develops basinwards. Most Niger Delta faulting is due to extensional deformation. The exception is in the distal section, where overthrust faults form in the toe of the proto-Niger delta. These extensional faults are normal and generally listric, comprising syndepositional growth faults and crustal tensional relief faults. These faults are synthetic or antithetic, running sub- parallel to the strike of the sub-basins. These synsedimentary faults exhibit growth strata above the down thrown block, as well as anticlinal (rollover) closures. Most hydrocarbon bearing structures in Niger Delta deposits are close to these structure-building faults, in complexly collapsed crest and faulted anticlinal structures. Growth faults and antithetic faults play an essential role in trap configuration. Growth fault exhibit significant throw (up to several hundred meters), are arcuate in plain view, concave basinward and may be several tens of kilometers in length.

1.3. Formations and Depositional Environments

The morphology of the Niger Delta changed from an early stage, spanning the Paleocene to Early Eocene, to a later stage of delta development beginning in Miocene time. Early coastlines were concave to the sea and depositional patterns were strongly influenced by basement topography [5]. Delta progradation occurred along two major axes. The first paralleled the Niger River, where sediment supply exceed subsidence rate. The second, smaller than the first, became active basinwards of the Cross River during the Eocene to Early Oligocene. Late stages of deposition began in the early to Middle Miocene, as these separate eastern and western depocentres merged. In late Miocene, the delta prograded far enough that shorelines became broadly concave into the basin. Accelerated loading by this rapid delta progradation mobilized underlying unstable shales. These shales rose into diapiric walls, deforming overlying strata. The resulting complex deformation structures caused local uplift, which resulted in major erosion events into the leading progradational edge of the Niger Delta. Several deep canyons, now clay filled, cut into the shelf are commonly interpreted to have formed during sea level low stands. The best known are the Afam, Opuama, and Qua Iboe Canyon fills [6,7]. Short and Stauble [1] defined formations within the Niger Delta clastic wedge based on sand/shale ratios estimated from subsurface well logs. The three major lithostratigraphic units defined in the subsurface of Niger Delta Akata, Agbada and Benin Formations reflect a gross upward-coarsening clastic wedge. These Formations were deposited in dominantly marine, deltaic and fluvial environments, respectively [3,8]. Stratigraphically equivalent units to these three formations are exposed in southern Nigerian [1]. The Akata Formation occur as prodeltaic dark grey shales and silts with rare streaks of sand of probable turbidite flow origin, is estimated to be 6,400m thick in the central part of this clastic wedge [1,5]. Marine planktonic foraminifera suggest a shallow marine shelf depositional setting ranging from Paleocene to Recent in age [5,9]. These shales are exposed onshore in the northeastern part of the delta, where they are referred to as the Imo shale. This formation also crops out offshore in diapers along the continental slopes, where deeply buried, Akata shales are typically over pressured. Akata shales have been interpreted to be prodelta and deeper water deposits that shoal vertically into the Agbada Formation [5,10]. It is thought to be the source rock of the Niger delta complex. The Agbada Formation occurs as a paralic sequence of shale and sand interbeds throughout the Niger Delta clastic wedge. It increases in shale thickness and decreases in sand thickness with depth. It has a maximum thickness of about 3,900m and ranges in age from Eocene to Pleistocene [5]. It crops out in southern Nigeria, where it is called the Ogwashi-Asaba and Ameki Formations respectively. The lithologies consist largely of alternating sands, silts and shales with progressive upward changes in grain size and bed thickness. The strata are generally interpreted to have formed in fluvial-deltaic environments [5,10]. The Agbada Formation underlies the Benin Formation and consists of interbedded fluvio-marine sands, sandstones and siltstone of various proportion and thickness representing cyclic sequence of offlap unit [8]. Texturally the sandstone vary from coarse to fine grained, poorly to very well sorted, unconsolidated to slightly consolidated. Lignite streak and limonite coating occur with some shell fragments and glauconites [1]. The shales are medium to dark grey, fairly consolidated and silty with localized glauconites. Shaliness increases downward and the formation pass gradually into the Akata formation. The Agbada Formation constitute a complex series of deposits laid down under at least five sub environments of deposition including holomarine, Barrier bar, barrier foot, Tidal coastal plain and lower deltaic flood plain [9]. The thickness ranges from 0-4500m.

The Benin Formation comprises the top part of the Niger Delta clastic wedge and described as the coastal plain sands which outcrop at the Benin-Onitsha area in the north to beyond the present coastline [1]. The top of the formation is the current sub aerially exposed delta top surface and its base is defined by the top of the youngest underlying marine shales, extends to a depth of about 1400m. The age of the formation is thought to range from Oligocene to Recent [1]. Shallow parts of the formation are composed entirely of non marine sands deposited in alluvial or upper coastal plain environment during progradation of the delta [5]. The formation thins basinward and ends near the shelf edge. The deposit is predominantly continental in origin and consist of massive, highly porous, fresh water bearing sandstones with localized clay drapes and little shale intercalation which increases toward the base of the formation. Texturally, it consists of fine grained sand and commonly granular. The grains are sub-rounded to well rounded, poorly sorted and partly unconsolidated. The sands are white or yellowish brown due to limonitic coat. Plant remains and lignite streak occur in places, with hematite and feldspar grain [8]. It ranges from Miocene – Recent in age; although lack of faunal content makes it difficult to date directly. The thickness ranges from 0 -2100m [1]. It is thickest in the central area of the delta where there is maximum subsidence. The Benin formation is partly marine, partly deltaic, partly estuarine and partly lagoonal or lay down in a continental upper deltaic environment [1]. The modern Niger Delta is a mixed wave, tide and fluvial deltaic system. The delta is reworked by wave action along an arcuate coast with barrier islands, back-barrier lagoons, and channel ridges. Thick mangroves border the coastline of the lower Niger Delta plain. Incised into this coastline are numerous tide-dominated coastal estuaries, that have gradually been filled with sediment following the Holocene sea level highstand. The modern delta front and continental slope is characterized by localized slumps and canyons that bypass sediments into deeper waters. Although details of deltaic features are difficult to decipher within reservoir intervals of Niger Delta deposits, the modern distribution of distributary channels, estuary fills, shoreface, back barrier lagoonal sediments, and delta plain deposits are assumed to be a good analog. It can be seen that the Niger delta has been affected by different episodes of progradation, retrogradation and aggradation as can be seen in the different sedimentation and especially in the Agbada formation. The Benin formation has been affected by a long period of progradation coupled with a regressive phase of the sea thereby creating accommodation space for deposition of continental clastics from the hinterland into the delta. Aggradational and paralic sequences of the Agbada formation are actually short lived phases between the transgressive phase and regressive phase of the sea thereby creating a non dominance stacking pattern in area where the sand to shale ratio is 50 percent. However with increasing dominance of the transgressive phase, the sand to shale ratio begins to reduce abruptly as more marine sediments tend to deposit and move towards the shores. In the continental slope and a little bit beyond the clastic wedge of the Niger delta sedimentary pile lies the prodelta of the Akata. Incised valley cut on the continental slope can create channels by which turbulent turbidity currents can move sediments down slope by gravity and sediments settles out by gravity in a turbidite sequence. Therefore the upper part of the Akata formation has lots of these isolated turbidite channel sand bodies underlain by continuous marine shale. These sand bodies are the objects for prospectivity in Niger delta deep water explorations.

1.4. Structural and Depositional History of Diapiric Shales

Diapiric shale structures began forming by Late Miocene time in response to lateral shale withdrawal from beneath the advancing deltaic load, combined with compressional uplift and folding of pro-delta strata. During the Pliocene and Pleistocene time, these structures were buried by the prograding delta and extensional growth faulting commenced. Subsidence within the depobelts ceased episodically, at which time alluvial sands advanced rapidly across the delta top, concurrent with a basinward shift in deposition and thereby creating seaward-stepping depocentres. Extensive gravity tectonism has deformed sediments over the continental slope and the resulting folding, faulting and diapirism have created intraslope basins 10 to 25 km wide, filled with thick sequences of ponded sediments that represent a wide range of depositional processes. Submarine canyons cut across these deformed zones and give rise to aggradational channel/levee systems which are distributaries for large deep-sea fans. Transport and deposition of terrigenous sediments beyond the shelf have been accomplished mainly by turbidites and mass transport deposits (slumps, debris flows). (Adapted from Nigeria - São Tomé & Príncipe Joint Development Authority November, 2004) The shale diapir belt spans from the western lobe of the Niger delta to the eastern lobe with only a thin representation where both lobes merged as can be seen in Figure 4, and Figure 5 respectively. These diapir zones are usually undercompacted and fluid laden which most often cause serious drilling problems. They cause abnormally high formation pressures and therefore special pore pressure analysts are usually employed when drilling through them.

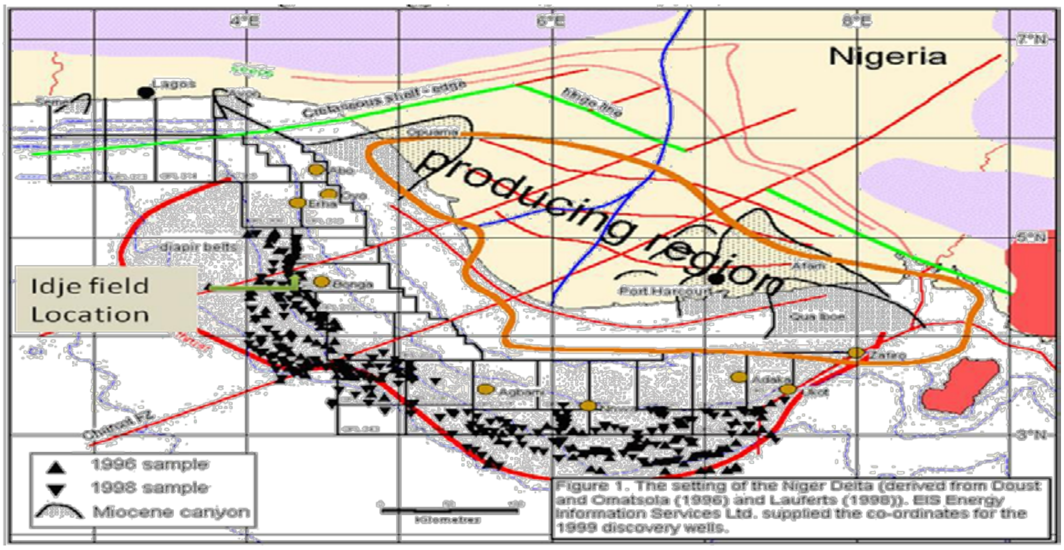

Figure 3. Niger – Delta structural setting [5] and Lauferts [11]

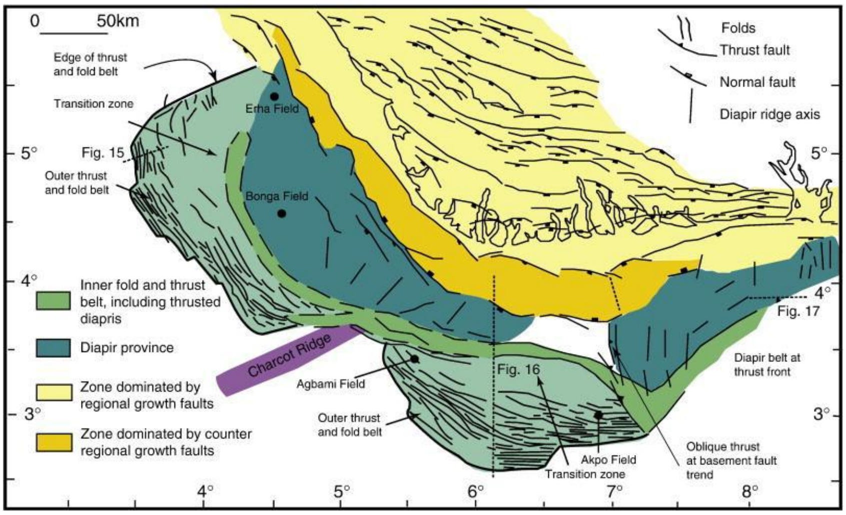

Figure 4. Regional map of Niger delta structural province (modified by [12])

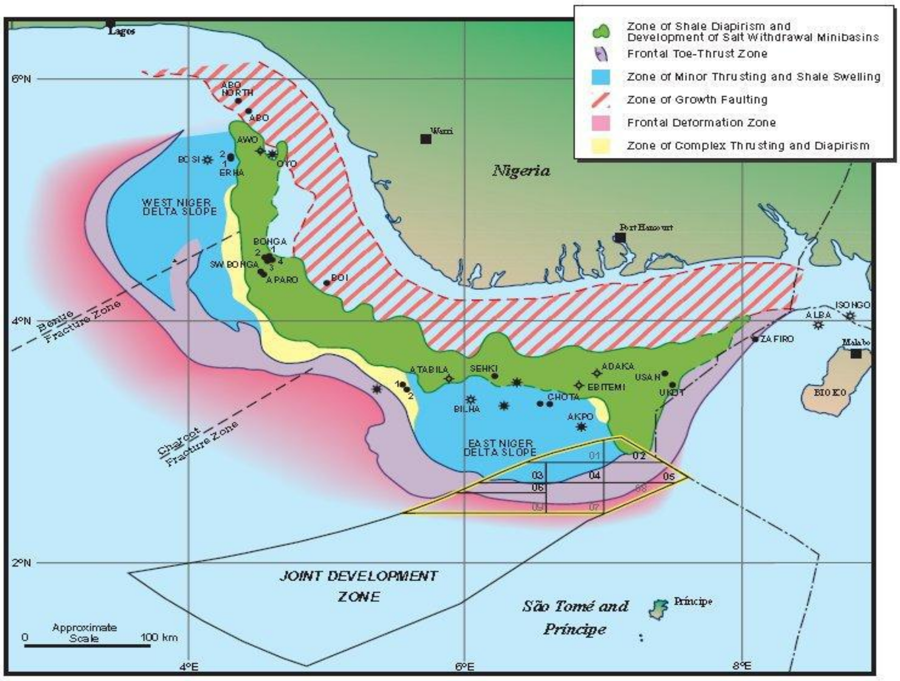

Figure 5. Tectonic map of Niger Delta (Adapted from Nigeria - São Tomé & Príncipe Joint Development Authority November 2004)

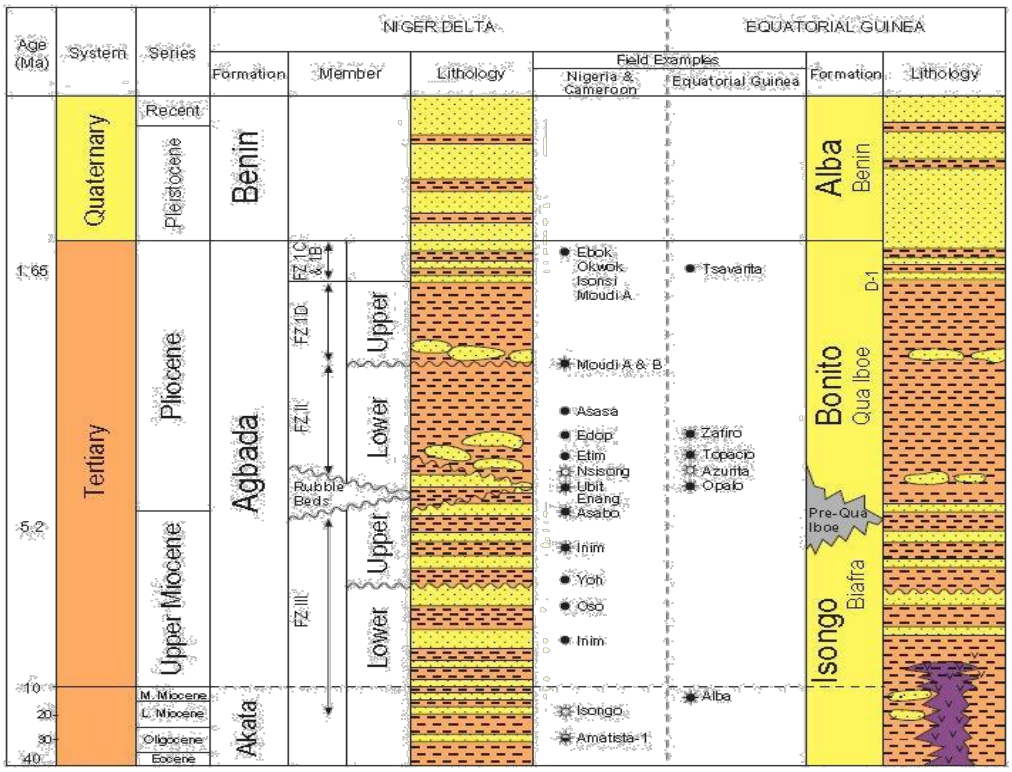

Figure 6. Niger Delta and Equatorial Guinea Stratigraphic Build up. (Modified from Equatorial Guinea Ministry of Mines and Hydrocarbon)

2. Materials and Methods

2.1. Data Overview

Idje field is located 70km southwest of Warri at the western lobe of Niger Delta. It lies within the proximal part of the deep offshore depobelt. The data used for this research include four wireline logs (gamma ray, resistivity, neutron and density) cutting across the same reservoir for ten wells in the field. The data set were obtained in ASCII format in softcopy. It was then uploaded in Schlumberger PETREL 2009 to generate continuous logs for the different wells. The reservoir properties were plotted with the use of Golden software SURFER 9 which gave contours by krigging techniques and also generated 3-D surfaces for the reservoir top.

2.2. Well Logs

Well logs are graphical measurements acquired by instruments lowered down a borehole on a wireline cable or drill pipe during or after drilling operation. During acquisition most measurements are made continuously whilst the instruments are moving. The resulting log of the measurements comprises a uniformly sampled set of data that is plotted against depth. Logs are an objective dataset that show how specific measurements vary within and between formation units. Well logs here for petrophysical analysis could be obtained from LWD (logging while drilling) data or from wireline logging data that could be cable conveyed or pipe conveyed.

2.2.1. Gamma-Ray Log

The gamma-ray logging device consists of an electrically operated, downhole counter that detects naturally occurring gamma rays. The gamma rays are detected as pulses that are transmitted to the surface where they are converted to electrical voltages and recorded continuously on film as the sonde is pulled up the hole. The rays are emitted by the unstable elements uranium, thorium, and potassium, which are found in measurable amounts in all rocks. Shale generally contains the greatest concentrations of these elements, and typically is more radioactive than sandstone, limestone, dolomite, salt, or anhydrite. Gamma-ray logging is thus highly useful in distinguishing shale from other rock types. Gamma-ray recording equipment is usually designed so that the curve deflects toward the right as radioactivity increases. On the gamma ray log, the deflection to the extreme right indicates shale. The parts of the curve with less deflection indicate non-shale lithologies such as sandstone and limestone. The gamma-ray log is used principally for bed definition, correlation, and determination of lithofacies because of its shale-distinguishing characteristic. The high penetrating power of gamma rays permits logging in cased or uncased holes, regardless of the nature of the fluid, if any, in the hole. The log is commonly calibrated from 0 to 150 API on a linear scale.

2.2.2. Resistivity Log

The resistivity log records the resistivities of subsurface formations and any fluids they may contain. Its design is based on electrical theory and instrumentation. The resistivity of the rock formation must be measured in the uncased portion of the borehole. Current and measuring electrodes are mounted on a mandrel or sonde and lowered down the hole. Different spacing between electrodes allows resistivity measurements at different distances from the borehole into the rock formation. A short spacing between electrodes gives a radius of investigation of only a few inches into the formation; longer spacing measures a larger radius. Three simultaneous resistivity measurements (micro, shallow and deep), using different electrode spacing, are usually recorded. The resistivities at different radii of penetration are compared to indicate the true resistivity, which is modified to varying degrees near the borehole by the invasion of the drilling mud into the rock and the influence of the borehole itself. The resistivity logs are calibrated on alogarithmic scale in ohm meters. High resistivity values are a direct indication of hydrocarbon bearing intervals. Gas and condensate resistivity values are relatively higher than those of oil. However resolution of fluid contact based on resistivity alone could be quite erroneous.

2.2.3. Neutron Log

The neutron log consists of an americium-beryllium or plutonium-beryllium source that emits fast neutrons, and a radiation detector placed close to the source. The emitted neutrons are electrically neutral particles that proceed outward from the source and penetrate into the adjacent rocks until they are captured by the atomic nuclei of certain elements after several collisions. When the neutron is captured, it is absorbed and one or more high-energy gamma rays are emitted. The induced gamma rays are of greater intensity and quantity than the naturally occurring gamma rays, thus permitting the measurements of the induced radiation without interference from the relatively weak, natural radiation. The atomic nucleus most successful in slowing down the emitted neutron is the hydrogen nucleus which has a mass almost identical to the neutron. When the hydrogen concentration is large, most of the neutrons are slowed down and captured within a short distance. Due to the source-detector spacing commonly used, a high concentration of hydrogen allows only a few gamma rays to reach the detector. Because hydrogen is a common component of formation fluids, and rocks must be porous to contain these fluids, the intensity of the induced gamma rays indicates the amount of fluid and porosity. High intensity generally signifies non porous rock, whereas low intensity signifies porous, fluid-bearing beds. Neutron is used to bombard the formation and the induced gamma ray from the bombardment is measured. The presence of hydrogen atoms tends to absorb the neutrons giving less room for gamma ray induction thus leading to low count rate. Shale generally shows a high porosity on a neutron log because of the hydrogen chemically combined in its molecules or present in water in its pores. The porosity, however, is not "effective porosity", as the voids are not interconnected, and shale is usually impervious. Natural gas, which contains less hydrogen than oil or water, gives a higher counting rate and the neutron curve records low, inaccurate porosity. The primary use of the neutron log is for porosity determination. It is also useful for delineation and correlation of formations. The log, like the gamma-ray log, can be made in either cased or uncased holes and requires no fluid. When used with the gamma ray, the neutron log may provide a quantitative record of shale and indicate porous and non-porous rock. Thus, it is particularly helpful in cased wells, for surveying old wells, and doing "work-over" jobs. Gas containing rocks may also be indicated. It is of interest to know here that neutron log only resolve the liquid filled pore spaces and give abnormally low porosity value for gas filled spaces. The neutron porosity could be calibrated in fractional porosity or in terms of percentage porosity. This work puts the fractional porosity calibration into consideration. It is calibrated from 0.7 on the left to 0 porosity units on the right i.e. it decreases to the right.

2.2.4. Density Log

The density log is acquired with a radioactivity tool based on the response of the rock to induced, medium-energy gamma rays. The result is an approximate measurement of the bulk density of the rock. The bulk density, as used in well logging, is the number of grams or mass weight of a substance divided by its volume. The tool consists of a gamma-ray source and a detector mounted on a skid that is in contact with the borehole wall. Gamma rays, which are emitted by the source, are transmitted through the formation. The number that reaches the detector depends on the abundance of electrons within the rock material. If many electrons are present, the gamma rays are quickly absorbed and only a few are counted. Conversely, if the electrons are few, many gamma rays are counted. An increase in counting rate therefore indicates a decrease in bulk density. Gamma ray from radioactive source is used to bombard rock and the reflected and diffused gamma ray is counted. Electrons tend to absorb the gamma ray and thus giving less count in the reflected gamma ray. The density log actually responds to electron density, but because the two densities are so closely related, the log is scaled in bulk density. Shales have a higher electron density than sand and thus its presence yields fewer counts than sand. The important relationship between the electron density as recorded by the density log and the porosity of a formation is simple and direct. A formation with a considerable amount of open space offers little resistance to the progression of medium-energy gamma rays. Therefore, rock with good porosity has a low electron and bulk density, as indicated by a high count of diffused gamma rays. The density log provides another method of direct porosity measurement. Oil and gas are less dense than water, which results in a lower density reading, and therefore, unlike a neutron log, their presence causes an indication of favorable porosity. When used to estimate effective porosity, the density log is not influenced as strongly by shale as the neutron log. The density log is calibrated from left to right and increases towards the right. The calibration used for the course of this project is from 1.65 to 2.65 g/cc.

2.3. Petrophysical Analysis

This involves the use of empirical formulae to estimate the petrophysical properties of the D-3 reservoir. The D-3 reservoir which was identified through the use of the electrofacies signatures were further characterized quantitatively to arrive at these petrophysical parameters, which include: volume of shale, formation factor, porosity, water saturation, permeability. Etc. Some of these parameters are discussed below:

2.3.1. Gamma Ray Index

The gamma ray log was used to determining the gamma ray index using the formula according to Asquith and Gibson, [13]:

$$I_{GR} = (GR_{LOG} - GR_{MIN})/(GR_{MAX} - GR_{MIN}) \quad (2.1)$$

Where,
I_{GR} = gamma ray index
GR_{LOG} = gamma ray reading of formation from log
GR_{MIN} = minimum gamma ray (clean sand)
GR_{MAX} = maximum gamma ray (shale)

2.3.2. Volume of Shale

The volume of shale was calculated by applying the gamma ray index in the appropriate volume of shale equation according to Larionov [14] for tertiary rocks:

$$V_{sh} = 0.083\left[2^{(3.7xIGR)} - 1.0\right] \quad (2.2)$$

Where,
V_{sh} = volume of shale
I_{GR} = gamma ray index.

2.3.3. Porosity

The computation of porosity was done in stages, the first involved the use of the Wyllie equation to estimate the density derived porosity (ϕ_D), and then the neutron-density porosity ($\phi_{N\text{-}D}$), was estimated using the neutron (ϕ_N) porosity coupled with the density derived porosity.

The Wyllie equation for density derived porosity is given as:

$$\phi_D = (\ell_{max} - \ell b)/(\ell_{max} - \ell_{fluid}) \quad (2.3)$$

Where:
density of rock matrix = 2.65 g/cc
ℓ_b= bulk density from log.
ℓ_{fluid} = density of fluid occupying pore spaces (0.74g/cc for gas, 0.9g/cc for oil and 1.1 g/cc for water)

The Neutron–Density porosity could be calculated according to

Shell/Schlumberger [15] as:

$$\phi_{N\text{-}D} = (\phi_N + \phi_D)/2$$

for oil and water column

$$\phi_{N\text{-}D} = (2\phi_D + \phi_N)/3$$

for gas bearing zones.

2.3.4. Formation Factor

This was achieved using the 'Humble' equation:

$$F = a/Ø^m \quad (2.6)$$

Where,
F=formation factor
a=tortuosity factor = 0.62
Ø= porosity
m = cementation factor = 2.15.

2.3.5. Formation Water Resistivity (Ωm)

Using the Archie's equation that related the formation factor (F) to the resistivity of a formation at 100% water saturation (R_o) and the resistivity of formation water (R_w), the resistivity of the formation water was estimated as:

$$R_w = R_o/F. \quad (2.7)$$

2.3.6. Water Saturation

Determination of the water saturation for the uninvaded zone was achieved using the Archie [16] equation given bellow:

$$S_w{}^2 = (F \text{ x } R_w)/R_T \quad (2.8)$$

But

$$F = R_o/R_w. \quad (2.9)$$

Thus,

$$S_w{}^2 = R_o/R_T. \quad (2.10)$$

Where
S_w=water saturation of the uninvaded zone
Ro=resistivity of formation at 100% water saturation
RT=true formation resistivity.

2.3.7. Hydrocarbon Saturation

This was obtained directly by subtracting the percentage water saturation from 100.

Thus:

$$S_{hy} = 1 - S_w.$$

Or

$$S_{hy}\% = 100 - S_w\% \quad (2.11)$$

Where, S_{hy} is the hydrocarbon saturation (expressed as a fraction or as percentage).

2.3.8. Resistivity Index

This was estimated using the ratio of formation true resistivity (R_t) to resistivity of formation at 100% saturation (Ro):

$$I = R_t / R_o \quad (2.12)$$

Where, '*I*' is the resistivity index. When *I* is equal to unity, it implies that the reservoir is at one hundred percent (100%) water saturation. The higher the value of '*I*', the greater the percentage of hydrocarbon saturation.

2.3.9. Bulk Volume Water

Bulk volume of water (BVW) was estimated as the product of water saturation (S_w) of the uninvaded zone and porosity ($Ø_{N\text{-}D}$). Thus,

$$BVW = S_w x Ø_{N\text{-}D} \quad (2.13)$$

Where, ØN-D= neutron-density porosity.

The hydrocarbon pore volume (HCPV) is the fraction of the reservoir volume occupied by hydrocarbon. This was calculated as the product of neutron-density porosity and hydrocarbon saturation as shown below:

$$\begin{aligned} HCPV &= Ø_{N-D} x (1 - S_w) \\ HCPV &= Ø_{N-D} x (S_h) \end{aligned} \quad (2.14)$$

2.3.11. Irreducible Water Saturation

The irreducible water saturation was calculated using the following relationship:

$$S_{wi} = (F / 2000)^{1/2} \quad (2.15)$$

Where,
S_{wi} = irreducible water saturation
F = formation factor.

However, this theoretical estimate of irreducible water is majorly useful in the estimation of relative permeability.

2.3.12. Permeability

This was based on the relationship between permeability, porosity, and irreducible water saturation according to Wyllie and Rose, [17]. The relationship is expressed as:

$$K = [(250 \text{ x } (Ø_{N-D})^3) / S_{wi}]^2 \quad (2.16)$$

2.3.13. V_{sh} Total

This is the total volume of shale represented as a depth factor within a well. It is calculated by:

$$Average\ V_{sh}\ x\ Gross\ thicknes \quad (2.17)$$

2.3.14. Net Thickness

This is the column of the reservoir that is occupied by reservoir formation (e.g. sand) only and exclusive of non reservoir formations (e.g. shale). It is calculated by:

$$Gross\ Thickness - V_{sh}Total \quad (2.18)$$

2.3.15. Net to Gross Ratio

This is the ratio between the net reservoir thickness and the gross reservoir thickness. However in terms of hydrocarbon pay, it could be calculated as the ratio between the net pay thickness and the gross pay thickness.

$$NTG = Net\ thickness \div Gross\ Thickness. \quad (2.19)$$

2.3.16. Effective Porosity

This is the porosity of the interconnected pore spaces. It assumes the absence of shale from the reservoir. It can be calculated using the following relationship:

$$\Phi effective = (1 - VSHALE) * \phi_{\text{N-D}} \quad (2.20)$$

2.3.17. Storage Volume

This is the capacity to store hydrocarbon in the reservoir. The storage volume is always higher than the hydrocarbon pore volume within a well because the net pay zone is inclusive of the grain matrix whereas, the grain matrix is absent in the hydrocarbon pore volume computation as only the hydrocarbon in the pore spaces is calculated for.

$$Storage\ Volume = \phi_{N-D} * Net\ Pay\ Thickness \quad (2.21)$$

2.3.18. Volume of Oil Resources

This is the volume of oil resources per unit acre in a field. It could be used to estimate oil reserve volume in the field.

$$Volume\ of\ Oil\ Resources = (7758 * h * HCPV) / B_o \quad (2.22)$$

Where h = net pay oil, B_o = Formation oil volume factor = 1.2 bbls/STB.

2.3.19. Volume of Gas Resources

This is the volume of gas resources per unit acre in a field. It could be used to estimate gas reserve volume in the field.

$$Volume\ of\ Gas\ Resources = (43560 * h * HCPV) / B_g \quad (2.23)$$

Where h = net pay gas, B_g = Formation gas volume factor = 0.005 cuft/scf.

2.3.20. Volume of Oil Originally in Place

Oil originally in place is computed with the following equation:

$$OOIP = Volume\ of\ Oil\ Resources * Area\ covered\ by\ oil \quad (2.24)$$

Here, recovery factors have not been applied. This volume could be calculated directly from the volume of oil resources contour map. The area of the map occupied by oil is calculated sectionally with respect to the contour intervals. The individual area is then multiplied by the individual contour value to get the individual volumes. Finally, all the individual volumes are added to get the total volume of oil resources in the field which is equivalent to the volume of oil in place. The unit here is stock tank barrels.

2.3.21. Volume of Gas Originally in Place

This is calculated the same way as that of oil originally in place from the volume of gas resources contour map. The unit here is standard cubic feet.

$$GOIP = Volume\ of\ Gas\ Resources * Area\ covered\ by\ gas \quad (2.25)$$

2.3.22. Direct Measurement of Hydrocarbon in Place

The hydrocarbon originally in place could also be computed directly using the average value for the net pay thicknesses, average hydrocarbon saturations, and average porosity values and substituted in the following equations:

$$OOIP = (7758 * A_{oil} * h_{oil} * s_{h(oil)} * \phi_{N-D}) / b_o \quad (2.26)$$

$$IP = (43560 * A_{gas} * h_{gas} * s_{h(gas)} * \phi_{N-D}) / b_g \quad (2.27)$$

A_{oil} = Area occupied by oil
A_{gas} = Area occupied by gas
h_{oil} = Average height of oil column
h_{gas} = Average height of gas column
$s_{h(oil)}$ = Hydrocarbon saturation (oil column)
$s_{h(gas)}$=Hydrocarbon saturation (gas)
NOTE: $1Km^2$ = 247.104 Acres

3. Results and Discussion

3.1. Petrophysical Table

The different petrophysical parameters computed for the D-3 reservoir are tabulated below:

Table 1. Petrophysical Table

	IDJE 1	IDJE 2	IDJE 3	IDJE 4	IDJE 5	IDJE 6	IDJE 7	IDJE 8	IDJE 9	IDJE 10
GR_I	0.1	0.25	0.34	0.23	0.31	0.29	0.24	0.06	0.08	0.32
^{V} SH	0.03	0.09	0.14	0.08	0.13	0.12	0.09	0.02	0.02	0.13
POROSITY (Ø)	0.26	0.25	0.24	0.26	0.25	0.25	0.26	0.26	0.26	0.24
F	11.63	12.41	12.22	11.3	11.06	11.17	11.38	11.42	11.44	12.09
^{R}w Ωm	0.1	0.09	0.09	0.1	0.1	0.1	0.1	0.1	0.1	0.09
S_w	0.71	0.21	0.21	0.94	0.94	0.89	0.97	0.97	0.97	0.18
^{S}hc	0.29	0.79	0.79	0.06	0.06	0.11	0.03	0.03	0.03	0.82
BVW	0.18	0.05	0.05	0.24	0.25	0.22	0.25	0.25	0.25	0.04
^{S}wirr	0.08	0.08	0.08	0.07	0.07	0.07	0.07	0.08	0.08	0.08
K mD	3516.94	2592.36	2564.57	3772.93	3737.13	3682.04	3820.48	3840.05	3854.89	2555.47
HCPV	0.08	0.2	0.19	0.02	0	0.03	0.01	0.01	0.01	0.2
TOP DEPTH ft	9410	9163	9170	9570	11262	9555	11251	11159	11188	9168
GOC ft	-	9381	9381	-	-	-	-	-	-	9381
OWC ft	9584	9584	9584	9584	-	9584	-	-	-	9584
BOTTOM DEPTH ft	9897	9613	9610	10011	11663	9977	11648	11649	11680	9598
GROSS THICKNESS ft	487	450	440	441	401	422	397	490	492	430
NET PAY THICKNESS ft	174	421	414	14	-	29	-	-	-	416
TOTAL V_{SH}	14.61	40.5	61.6	35.28	52.13	50.64	35.73	9.8	9.84	55.9
NET THICKNESS ft	472.39	409.5	378.4	405.72	348.87	371.36	361.27	480.2	482.16	374.1
N/G RATIO	0.97	0.91	0.86	0.92	0.87	0.88	0.91	0.98	0.98	0.87
^{POROSITY}EFFECTIVE	0.25	0.23	0.21	0.24	0.22	0.22	0.24	0.25	0.25	0.21
STORAGE VOLUME	45.24	105.25	99.36	3.64	-	7.25	-	-	-	99.84
VOL OF OIL RESOURCES	89992.8	262479	249355.05	1810.2	-	5624.55	-	-	-	262479
VOL OF GAS RESOURCES	-	379843200	349264080	-	-	-	-	-	-	371131200

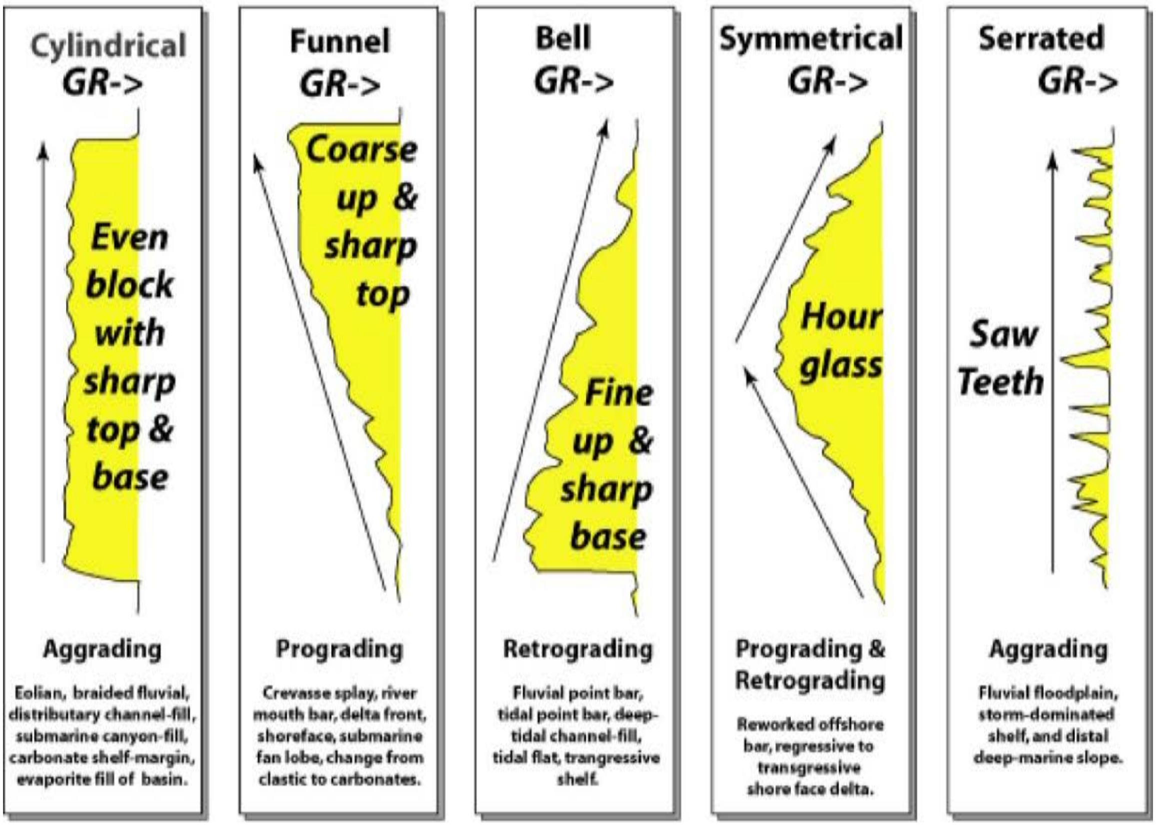

Figure 7. Interpreting depositional environment using gamma ray log motifs [18]

3.2. Log Shape and Inferred Environment

Deductions from the log motif and results from petrophysical evaluation culminated in interpretation that the inferred environment ranges from slope channel or submarine canyon fill (even block with sharp top and base, [18] (Figure 7) in the western part of the map area to the distal deep marine slope (serrated edges) towards the eastern portion.

3.3. Well Correlation

Correct interpretation of log is critical to any reservoir evaluation and characterization. Log correlation provides the basis for the determination of reservoir geometry and architecture. [19]. Three sets of correlations were made on Idje field, E-W (Figure 9), NE-SW (Figure 10) and NW-SE (Figure 11) using a combination of the unique electrofacies suites across the clean D-3 reservoir coupled with the lateral fluid contacts across the wells in the central portion of the dome and the results indicates that the accumulation of hydrocarbon in the D-3 reservoir is in the centre of a localized sedimentary dome with a 4-way dip closure in all directions. The facies association as represented by the increasing degree of shaliness towards the eastern part of the field, and inferred progression from the proximal to the distal portion of the slope, clearly indicates the direction of localized depositional dip. The Idje slope channel therefore dips from west to east as opposed to the Niger Delta regional dip of NE-SW trend.

Table 2. Standard Porosity and Permeability Table [20]

Percentage Porosity (%)	Qualitative Description	Average K_Value (md)	Qualitative Description
0-5	Negligible	<10.5	Poor to fair
5-10	Poor	15-50	Moderate
15-20	Good	50-250	Good
20-30	Very Good	250-1000	Very Good
>30	Excellent	>1000	Excellent

Table 3. Classification of Sandstone reservoir based on shale content [19]

Classification of sandstone reservoir based on shale contents	
Clean sand	<5% Vshale
Slightly shaly sand	5-15% Vshale
Shaly sand	15-25% Vshale
Very shaly sand	25-35% Vshale
shales	>35% Vshale

[19].

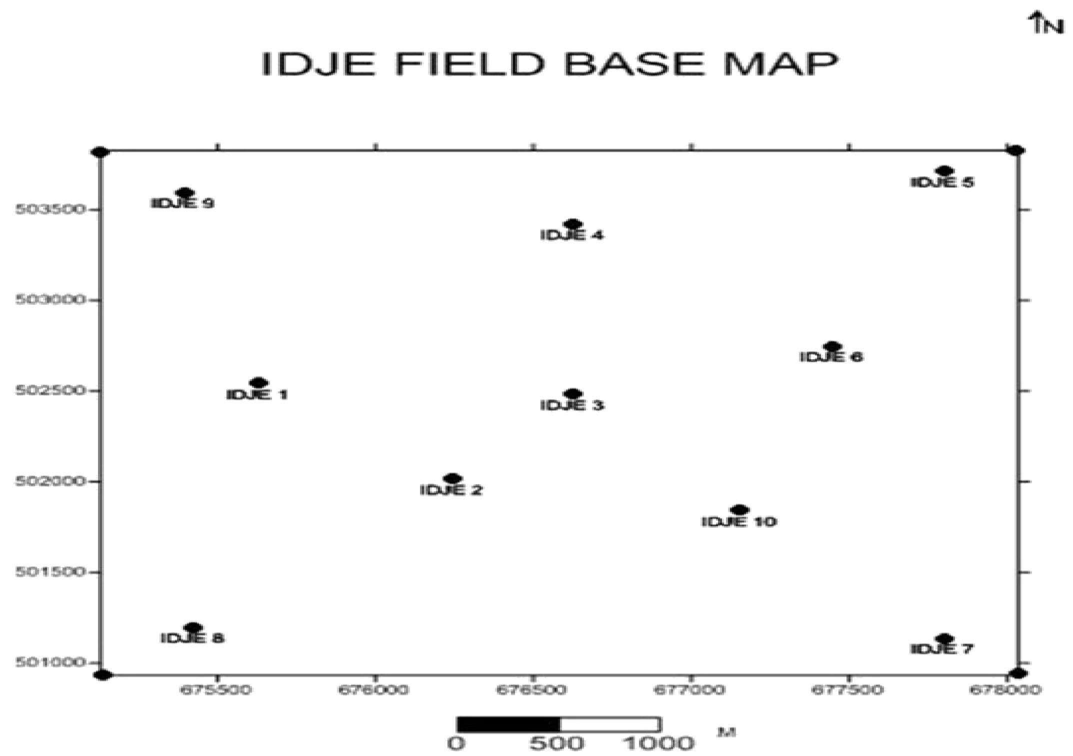

Figure 8. Idje Field Base Map in Utm Coordinates

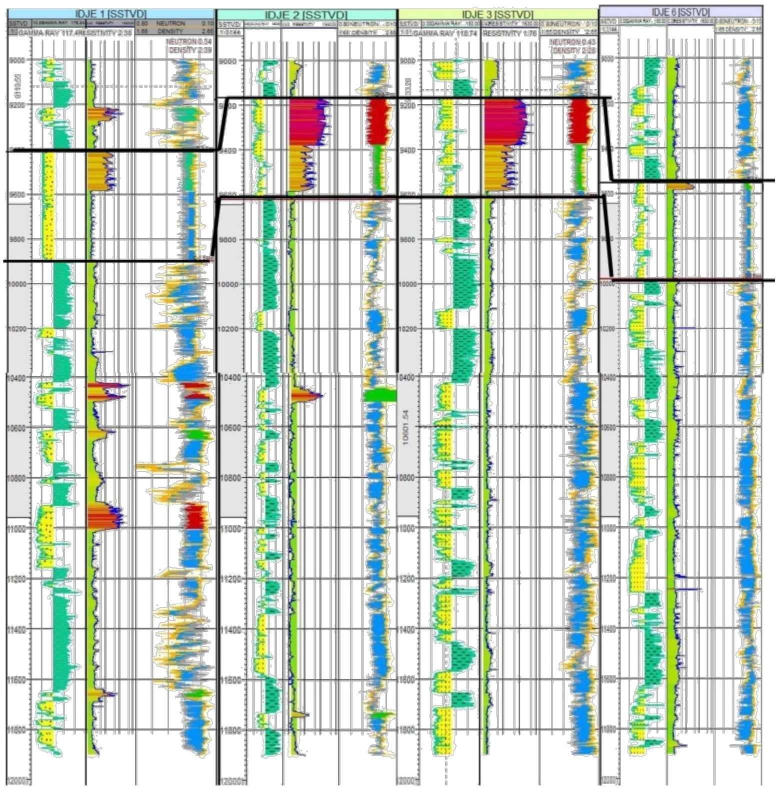

Figure 9. E-W Correlation

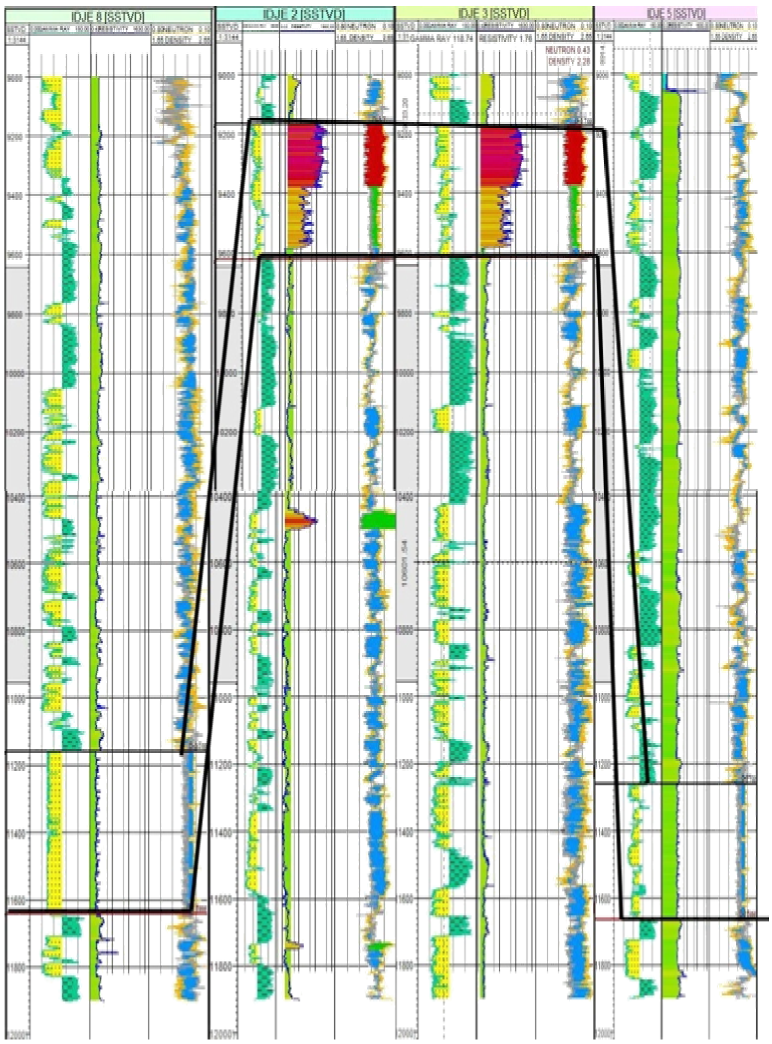

Figure 10. NE – SW Correlation

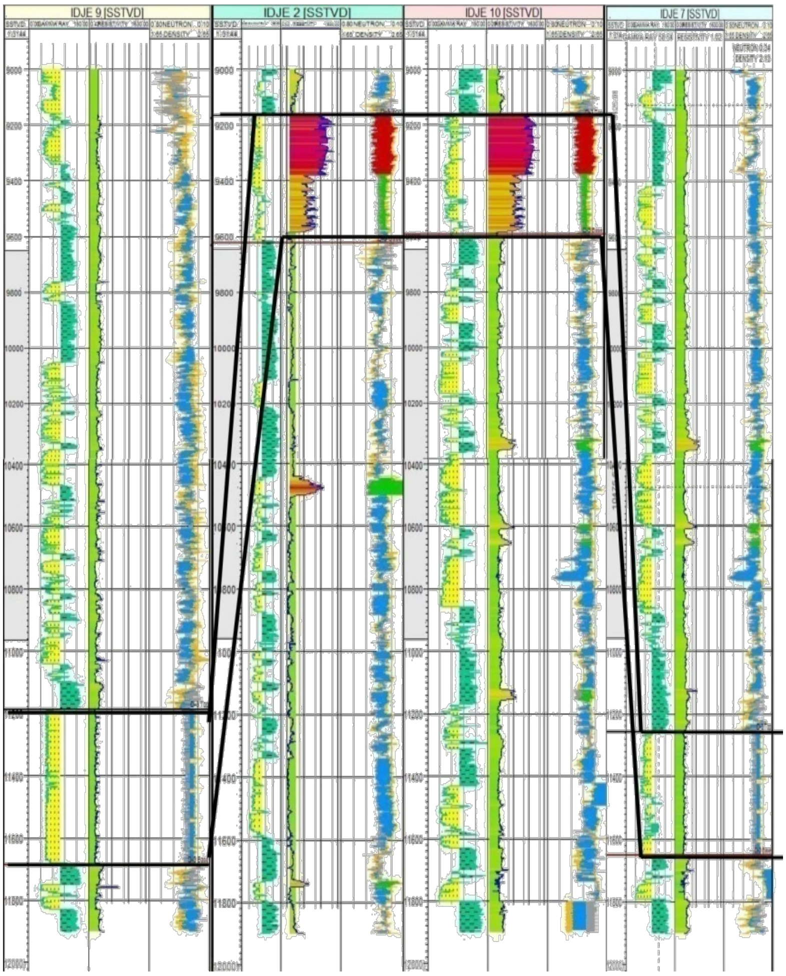

Figure 11. NW-SE correlation

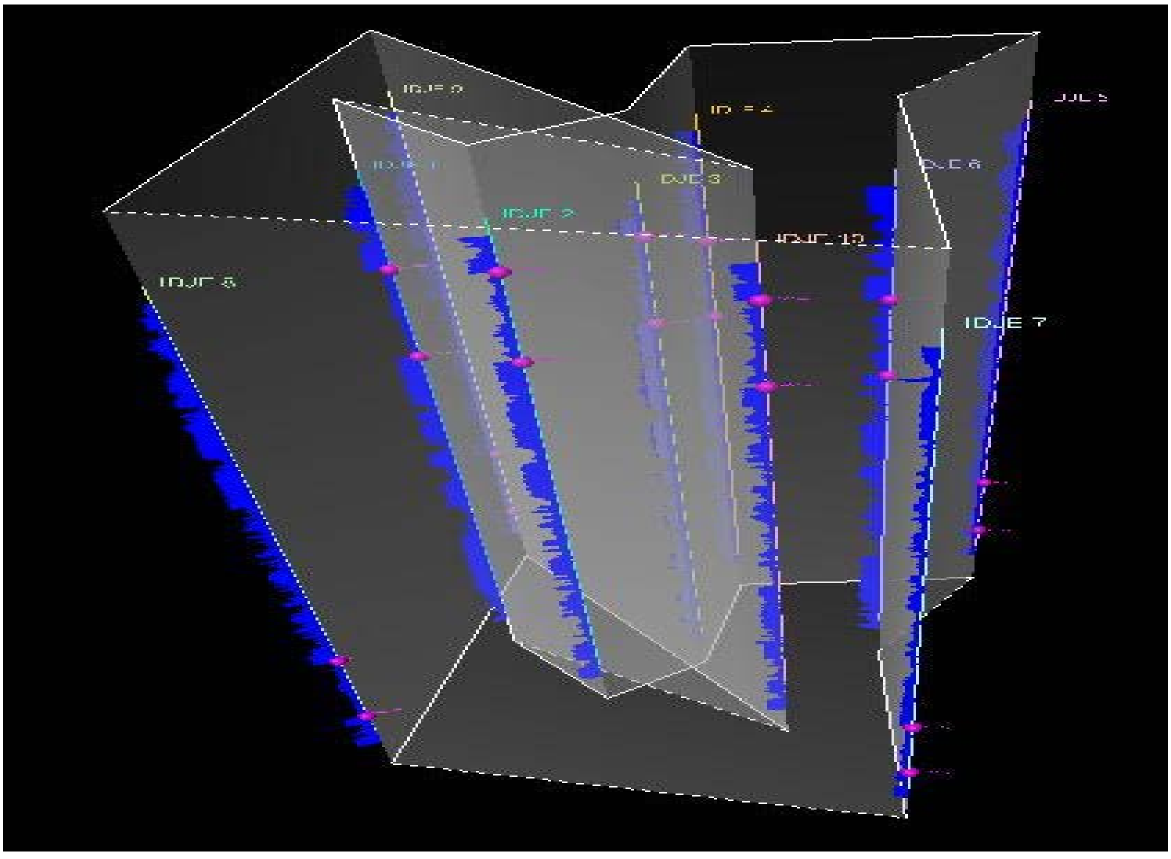

Figure 12. 3 – D View of Idje Wells Showing the D-3 Horizon

The E-W correlation was done using Idje 1, 2, 3 and 6. Although Idje 1 and 6 are not gas bearing, the oil water contacts are the same as the gas bearing Idje 2 and 3 and therefore indicated the oil bearing portion of the reservoir.

The NE-SW correlation was done using Idje 8, 2, 3 and 5. However due to the distance of Idje 8 and 5 from the crest of the dome coupled with their relative lower elevation from the fluid contacts, they have been shown to be sited in the water bearing portion of the reservoir.

The NW-SE correlation followed similar trend as the NE-SW correlation. However it was done using Idje 9, 2, 10 and 7 respectively with Idje 2 and 10 in the oil and gas bearing portion and Idje 9 and 7 only in the water portion.

The intersection of the three correlation trends gives the crest of the structural dome with radial dip closures.

Figure 13 shows the 3-D surface of the reservoir top with the various fluid contacts. The gas-oil contact is seen at 9831ft while the oil-water contact is at 9584ft respectively. The hydrocarbon is shown to occupy the central part of the map area and radially surrounded by water indicating its entrapment in the central portion of the structural dome.

From Figure 12, it was seen that the wells at the flanges of the map areas have the D – 3 reservoirs at the bottom of the wells whereas those at the central portion of the map area have the D-3 reservoir at the top of the wells. This clearly indicated that the reservoir has structural dome architecture.

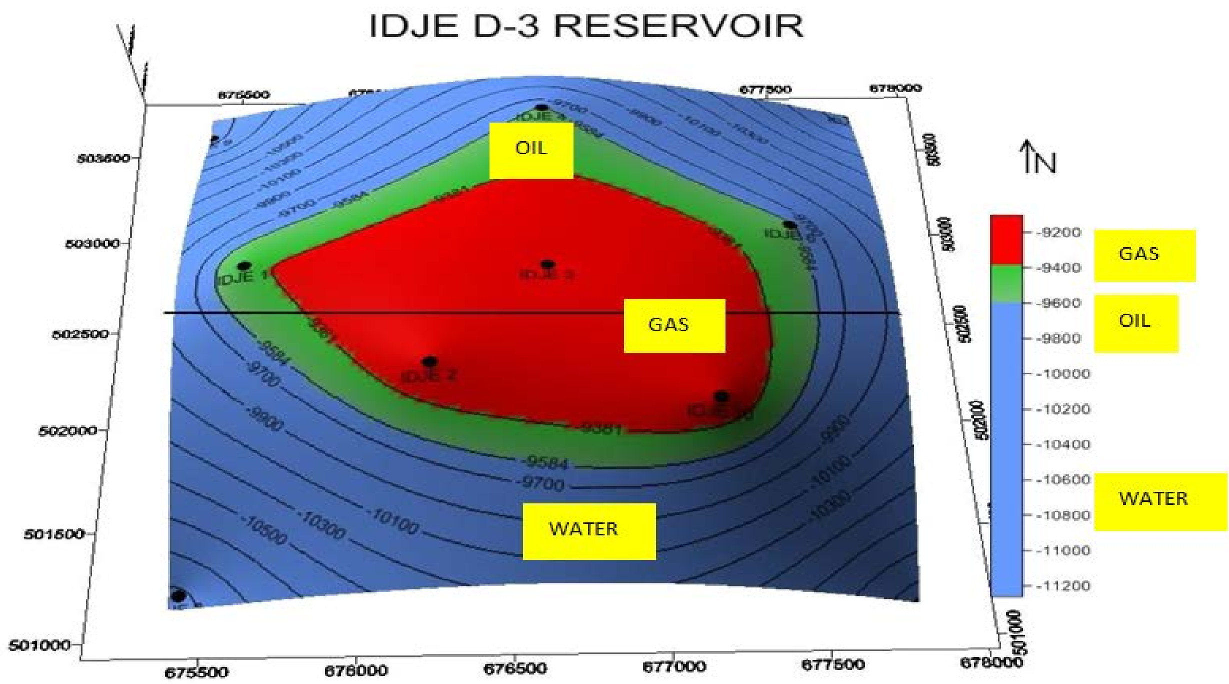

Figure 13. 3-D Contour Map of D-3 Reservoir Top

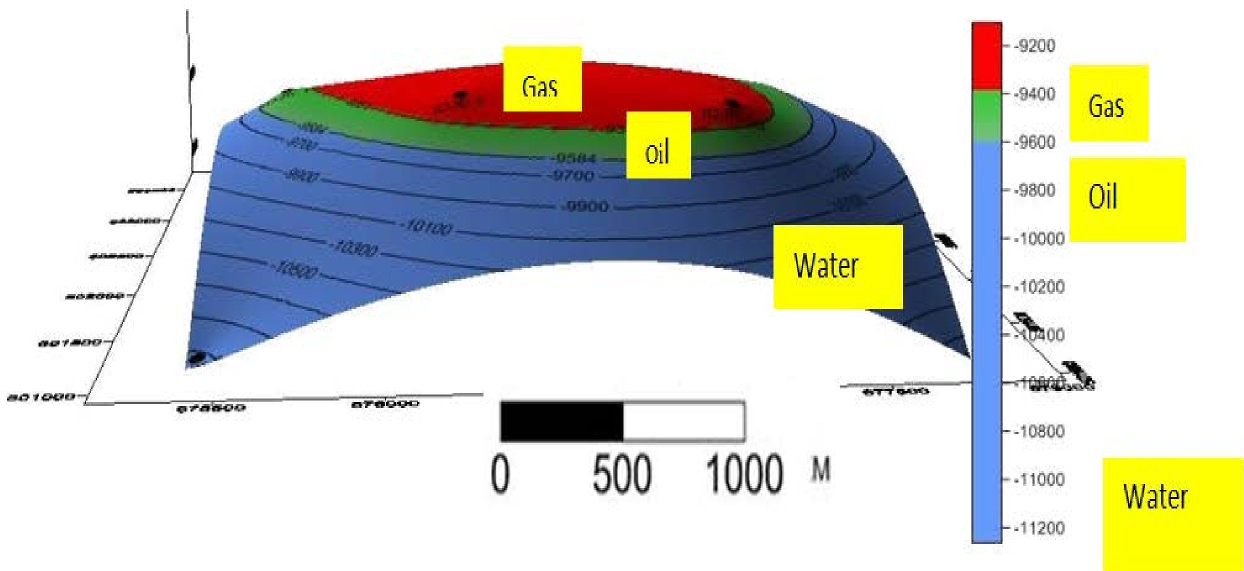

Figure 14. E – W Cross Section of Idje D-3 Reservoir

The D-3 reservoir had been shown to have been deposited in a slope channel or a submarine canyon fill in the proximal western portion to a distal deep marine slope (Figure 7) towards the eastern portion of the basin. The reservoir is shown to have very good porosities and excellent permeabilities (Table 2) with average porosity of 0.25 and average permeability of 3393.69mD respectively. The D-3 reservoir has relatively low irreducible water saturation. The porosity and effective porosity values across the reservoir have very close similarities. The net to gross ratio is also relatively very high. These are direct indications that the reservoir has very good interconnected pore spaces and is symptomatic of the locally high permeability values as against the 1 – 2 Darcies of the Niger Delta permeability range [21]. It has good hydrocarbon saturation and therefore huge prospect for hydrocarbon production. The low irreducible water saturation would account for a low water saturation cut-off to be employed when considering production well citing. There is every tendency to produce water alongside the hydrocarbon and thus measures for separation must be put in place unless the water saturation cut-off is less than or equal to the irreducible water saturation. The reservoir is also shown to range in sand thickness from clean sand in the western portion to slightly shaly sand (Table 3) in the eastern portion indicating progressively finer grains as you go further basinward indicating direction of lithologic dip. Structural correlations have revealed the D-3 reservoir architecture to be a sedimentary dome with reduced porosities and permeabilities at the crest of the dome. The structural dome could be resulting from localized shale/clay diapirs on the Niger Delta continental slope region.

4. Conclusion

This work could be used as an input tool for pre existing models to generate excellent dynamic simulations for optimum productivity. Water saturation, irreducible water saturation, porosity, permeability and hydrocarbon saturation combined could be used to give advice on possible locations to site water injection wells and drain holes for further field development.

This work could also be incorporated into a number of multi-disciplinary projects that use integrated subsurface datasets (core, wireline log, 3D seismic and production data), insights from outcrop analogues and novel modeling techniques to characterize Geology and fluid flow in hydrocarbon reservoirs.

Acknowledgements

The authors express their profound appreciations to the Geoscience team at Ciscon Nigeria Limited, Warri and Prof. A.I. Igbafe.

References

[1] Short, K.C, and A.J. Stauble, 1967. Outline of Geology of Niger Delta: American Association of Petroleum Geologists, Bulletin, v.51, p.761-779.

[2] Avbovbo, A.A, 1978. Tertiary lithostratigraphy of Niger Delta: Amer. Assoc Petrol. Geol. Bull., V. 62, p 295-306.

[3] Weber, K.J, and Daukoru, E.M, 1975. Petroleum Geology of the Niger Delta: Proceedings of the Ninth World Petroleum Congress, volume 2, Geology: London, Applied Science Publishers Ltd., p.210-221.

[4] Evamy, B. D; Haremboure, J; Kamerling, P; Knaap, W.A; Molloy, F.A; and Rowlands, P.H, 1978. Hydrocarbon habitat of Tertiary Niger Delta: American Association of Petroleum Geologists Bulletin, v.62, p. 77-298.

[5] Doust, H, and Omatsola, E, 1990. Niger Delta, in, Edwards, J.D., and Santogrossi, P.A., eds., Divergent/passive Margin Basins, AAPG Memoir 48: Tulsa, American Association of Petroleum Geologists; p.239-248.

[6] Reijers, T.J.A; S.W, Petters, and C.S, Nwajide, 1997. The Niger Delta Basin, inR.C. Selley, ed., African Basins-Sedimentary Basin of the World 3, Amsterdam, Elsevier Science, p.151-172.

[7] Tuttle, W.L.M; Charpentier, R.R; and Brownfield, M.E, 1999. The Niger Deltapetroleum system; Niger delta province, Nigeria, Cameroon and Equatorial Guinea, Africa USGS. Denver, Colorado, open file report, world energy project.

[8] Weber, K.J, 1987. Hydrocarbon distribution patterns in Nigerian growth faultsstructures controlled by structural styles and stratigraphy: Journal of Petroleum Science and Engineering. V. 1, p. 91-104.

[9] Whiteman, A, 1982. Nigeria: Its Petroleum Geology, Resources and Potential:London, Graham and Trotman, p. 110-160.

[10] Stacher, P, 1995. Present Understanding of the Niger Delta hydrocarbonhabitate. In: M. N Oti and G. Postman Eds. Geology of Deltas. AA Balkema, Rotterdam. Pp 257-267.

[11] Lauferts, H. 1998. "Deep Offshore West Niger Delta Slope, Nigeria - Scale and Geometries in Seismic and Outcrop Indicating Mechanisms for Deposition". Extended Abstracts. AAPG International Conference and Exhibition. 18 - 19.

[12] Morley, 2010. Deepwater fold and thrustbelt classification, tectonics, structureand hydrocarbon productivity: A review

[13] Asquith, G.B, and Gibson, C.R, 1982. Basic Well Log Analysis for Geologists. 3rd Printing, Published by American Association of Petroleum Geologists, Tulsa Oklahoma USA. 216pp.

[14] Larionov, V.V., 1969. Borehole Radiometry: Moscow, U.S.S.R., Nedra.112P in Asquith, G. and Krygowski, D., 2004. Basic Well Log Analysis. AAPG Methods in Exploration Series v. 16, 204p.

[15] Shell/Schlumberger, 1999. Petrophysics Distance Learning. Hague, Netherlands.

[16] Archie, G.E, 1942. The electrical resistivity log as an aid in determining somereservoir characteristics. Journal of Petroleum Technology, 5, pp. 54-62.

[17] Wyllie, M.R.J. and W.D. Rose. 1950. "Some Theoretical Considerations Related to the Quantitative Evaluations of the Physical Characteristics of Rock from Electric Log Data". Journal of Petroleum Technology. 189:105-110.

[18] Kendall C (2003) Use of well logs for sequence Stratigraphic interpretation of the subsurface. USC Sequence stratigraphy web. http://strata.geol.sc.edu/index.html. University of South Carolina.

[19] Davies, D.K, 2002. Foundation of Petrophysics. Petroskills Training, Vol B.

[20] Etu-Efeotor, J.O, 1997. Fundamentals of Petroleum Geology. Published byParagraphics (an imprint of Jeson services) .Port Harcourt. Pp.62, 64, 146.

[21] Omatsola, M.E, 1982: Petroleum Geology of Niger Delta. Shell International Petroleum Nigeria. The Hague, Netherlands.